Quantum Electronics **33** (11) 1009 – 1014 (2003)

CONTROL OF LASER RADIATION PARAMETERS

PACS numbers: 42.55.Rz; 42.60.Fc
DOI: 10.1070/QE2003v033n11ABEH002541

Evolution of the shape and spectrum of ultrashort pulses upon active mode locking

V.A. Zaporozhchenko

***Abstract*. Time sweeps of the autocorrelation function and the emission spectrum of an actively mode-locked Nd : YAG laser are recorded during the development of quasi-continuous pre-lasing maintained by a negative feedback loop. It is found that higher Hermitian – Gaussian supermodes are present at the transient stage of radiation, and the ultrashort pulse shortening is accompanied by the shift of the lasing spectrum to the red wing of the gain band of the active medium.**

Keywords: *mode locking, autocorrelation function, supermodes.*

1. Introduction

The process of nonstationary formation of ultrashort pulses in mode-locked lasers attracted attention already when flashlamp-pumped pulsed solid-state lasers were virtually the only sources of picosecond light pulses. First Letokhov [1] and then Kuizenga and Siegman [2, 3] considered the evolution of a pulse circulating in a laser resonator and experiencing both shortening under the action of a modulator and dispersion broadening in an active medium. According to the theory, to achieve the pulse duration close to the stationary limit, from 200 up to a few tens of thousands of transits of radiation in the resonator are required, depending on lasing parameters.

The presence of a rather long transient stage of formation of ultrashort pulses in actively mode-locked lasers became the main obstacle for generating transform-limited pulses with reproducible parameters in Q-switched lasers because in this case lasing develops much faster than mode locking is established. For this reason, in most laser systems the pre-lasing formation of ultrashort pulses was employed by using stepwise Q-switching [4] or negative feedback maintaining quasi-stationary pre-lasing for a quite long time [5, 6]. The basic conclusions of the theory were indirectly experimentally confirmed during investigations of such laser systems.

An attempt to measure directly the dependence of the pulse duration on its formation time in a rapidly Q-switched laser was made in Ref. [3]. Pre-lasing in a laser stabilised by a negative feedback loop in the presence of frequency jitter comparable to the ultrashort-pulse formation time was studied in Ref. [7]. The measurement [8] of the time sweep of the pre-lasing autocorrelation function (ACF) for this laser with a time resolution of 50 ns showed that the stationary duration of ultrashort pulses was established already by the instant of the detection threshold. However, a mode locker was switched in Ref. [8] long before the lasing threshold achievement, resulting in the formation of ultrashort pulses in the resonator with $\sim 60\,\%$ losses per transit before the threshold achievement. This was neglected in the analysis of experimental data, which were erroneously interpreted as an evidence of a rapid formation of ultrashort pulses.

In this paper, the transient process of ultrashort pulse formation was studied by recording the time sweep of the ACF in an actively mode-locked Nd : YAG laser. A mode locker was switched simultaneously with the beginning of detection upon the lasing threshold achievement. This corresponded to the initial conditions, which were used in the theoretical analysis [1, 3] of transient processes of formation of ultrashort pulses. Simultaneously, the evolution of the laser emission spectrum was studied. The experimental data obtained in the case of the reproducible, as shown in Ref. [9], dynamics of pre-lasing at long (up to 100 μs) time intervals allow one to describe the evolution of radiation in mode-locked lasers in more detail.

2. Laser and the detection system

In the experiment, shown schematically in Fig. 1, a laser with a resonator formed by highly reflecting mirrors – flat (*8*) and spherical (*2*) with the radius of curvature equal to 2.5 m, was used. The resonator contained active element (*7*) ($\varnothing 3 \times 65$ mm), acoustooptic modulator (*3*), polariser (*5*), and two electrooptical DKDP crystals, one of them (*6*) in the negative feedback loop and another (*4*) could be used to couple out a single pulse of the resonator. The laser operated upon flashlamp pump without Q-switching, and quasi-continuous pre-lasing was maintained by the negative feedback loop during ~ 100 μs. A part of radiation coupled out of the resonator by a polariser, at a 1.7-kV constant voltage applied to electrooptical crystal (*6*), was used to control the negative feedback via photodiode (*9*); the remained radiation was directed to the detection system.

The modulator was controlled by a radio pulse with a peak power of ~ 30 W, which provided almost a 100 % modulation degree. A radio pulse was fed to the modulator at the instant of the appearance of a timing pulse, which was

V.A. Zaporozhchenko B.I. Stepanov Institute of Physics, National Academy of Sciences of Belarus, prosp. F. Skoriny 68, 20072 Minsk, Belarus; e-mail: vzap@dragon.bas-net.by;
web-site: http://ifanbel.bas-net.by/

Received 18 December 2002; revision received 18 March 2003
Kvantovaya Elektronika **33** (11) 1009 – 1014 (2003)
Translated by M.N. Sapozhnikov

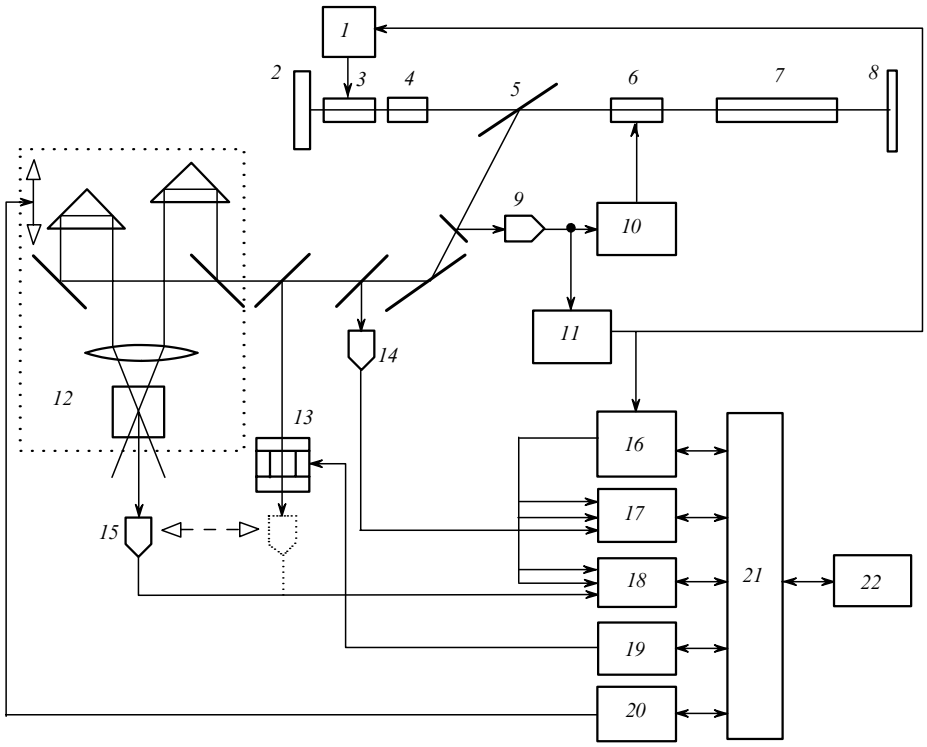

Figure 1. Experimental setup: (*1*) radio pulse shaper; (*2*, *8*) mirrors; (*3*) modulator; (*4*, *6*) electrooptical crystals; (*5*) polariser; (*7*) active element; (*9*, *14*, *15*) photodiodes; (*10*) negative feedback amplifier; (*11*) comparator; (*12*) autocorrelator; (*13*) scanning interferometer; (*16*) strobe oscillator; (*17*, *18*) analogue-to-digital converters; (*19*) digital-to-analogue converter; (*20*) optical delay control unit; (*21*) CAMAC; (*22*) computer.

formed by fast comparator (*11*) monitoring the output signal of photodiode (*9*). The same pulse triggered the detection system comprised of two analogue-to-digital converters (*17*) and (*18*) with the time constant equal to 50 ns, which were synchronised at the frequency 10 MHz from common generator (*16*). This provided the time resolution of 100 ns and the synchronous normalisation of signals. The use of a comparator to lock the time sweep of signals to the development of oscillation in the laser eliminated the jitter influence on the averaging of the results of evolution measurements. All the measurements were performed using averaging over an ensemble of 100 laser pulses.

The time parameters of ultrashort pulses were analysed with autocorrelator (*12*), which was based on a noncollinear SHG and controlled by computer (*22*) through CAMAC line (*21*) and control module (*20*). One of the fast photodiodes (*14*) detected radiation at the fundamental frequency at the input of the measuring system and the second one (*15*) detected second-harmonic radiation at the correlator output. The SHG efficiency $\eta(T,\tau) = P_{2\omega}(T,\tau)/P_{\omega}^2(T)$ was calculated for each laser pulse and each of the 1024 time slices of signals and then was averaged over an ensemble of 100 measurements (T is the time measured in the round-trip transit time of radiation in the resonator, and τ is the time delay in the correlator).

The laser emission spectrum was analysed with a Fabry–Perot interferometer (*13*), which was scanned with the help of digital-to-analogue converter (*19*). In this case, radiation was detected at the input and output of the interferometer and its transmission $\xi(T,\delta) = P_{\text{out}}(T,\delta)/P_{\text{in}}(T)$ was calculated depending on the phase difference δ determined by the interferometer base. It is well known [10] that the measurements of the width and shape of the ultrashort pulse spectrum using a Fabry–Perot interferometer are hindered because of a too broad instrumental contour; however, interferometric measurements give correct information on the central frequency of radiation and its shift during the development of lasing.

The length of the laser resonator was adjusted by the maximum SHG efficiency at the zero optical delay $\eta(T,0)$ in the autocorrelator at the values of T corresponding to the established mode locking regime. This provided the minimum duration of laser pulses. The mismatch between the modulation frequency and intermode beat frequency was not controlled.

3. Results of measurements

The time sweeps of the ACF and the laser emission spectrum are shown in Fig. 2. At the initial stage of the ultrashort pulse formation, a distinct structure is observed, first having five and then three maxima, which are smoothed with decreasing the ACF half-width (Fig. 2a). The shortening of the pulse duration is accompanied by a continuous shift of the emission spectrum to the red (Fig. 2b). Figure 3 shows the time dependences of the main parameters of radiation, which allow one to analyse the type of transient processes in an actively mode-locked laser.

Figure 3a shows the envelope of the laser pulse energy. A rather large oscillation amplitude compared to that observed earlier in Ref. [9] is caused by a deliberate reduction of the transfer coefficient of the negative feedback loop in order to increase the output pre-lasing power and to provide the corresponding expansion of the dynamic range of the measuring system. An almost complete suppression of

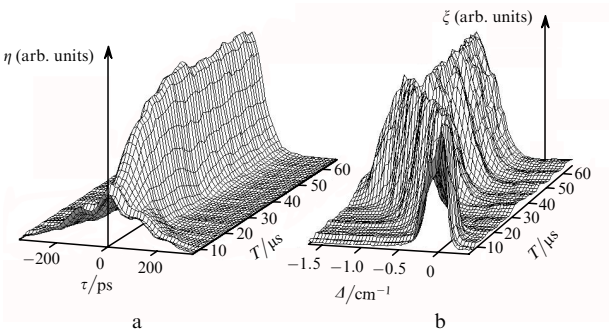

Figure 2. Time sweeps of the autocorrelation function (a) and emission spectrum (b).

lasing during first several microseconds is caused by the switching of the modulator, which introduces noticeable losses (more than 50 %) to radiation filling uniformly the resonator. Only after shortening of the duration of a pulse circulating in the resonator, these losses become insignificant.

Lasing appears again approximately within 5 μs after modulator switching. In this case, the ACF half-width $\tau_{1/2}$ monotonically decreases (Fig. 3b) and the emission spectrum shifts (Fig. 3d). Already after 15 μs, the pulse duration exceeds the stationary value only by 20 %, and it further decreases for 15 – 20 μs almost unnoticeably. This stage of the establishment of mode-locking regime is more clearly demonstrated by the increase in $\eta(T, 0)$ (Fig. 3c) and he shift of the emission spectrum (Fig. 3d). Finally, within 40 μs after modulator switching (4000 transits of a circulating pulse in the resonator), a stationary regime is established for a circulating pulse in the resonator, when the duration and spectrum of the ultrashort pulse do not change during its transits in the resonator despite strong variations in its energy.

Noteworthy is the behaviour of the lasing parameters within 35 – 40 μs after the instant of modulator switching and directly before the establishment of the stationary regime. At this time, the shift of the spectrum exceeds the stationary value, the SHG efficiency is maximal, and the ACF half-width is minimal. It is in this region of the transition to the stationary regime that the ACF shape is most close to a Gaussian pulse with the FWHM duration equal to 67 ps. Later, in the stationary regime, the ACF is better approximated by a pulse with the envelope in the form of hyperbolic secant of almost the same duration (Fig. 4a). Such behaviour was observed in different series of experiments with different modulation parameters and the transfer coefficient of the negative feedback loop. An increase in the modulation degree resulted in the appearance of a dip in the train envelope at this instant, up to an almost complete suppression of lasing for a few microseconds.

4. Shape of the autocorrelation function and 'supermodes'

A number of details of the time sweep of the ACF in Fig. 2a deserve special attention. The ACF shape at the beginning of the sweep cannot be described using the evolution approach to the analysis of active mode locking employed in Refs [1 – 3], but it is too characteristic to be interpreted as a manifestation of a noise background near a pulse being formed. Such an interpretation would require

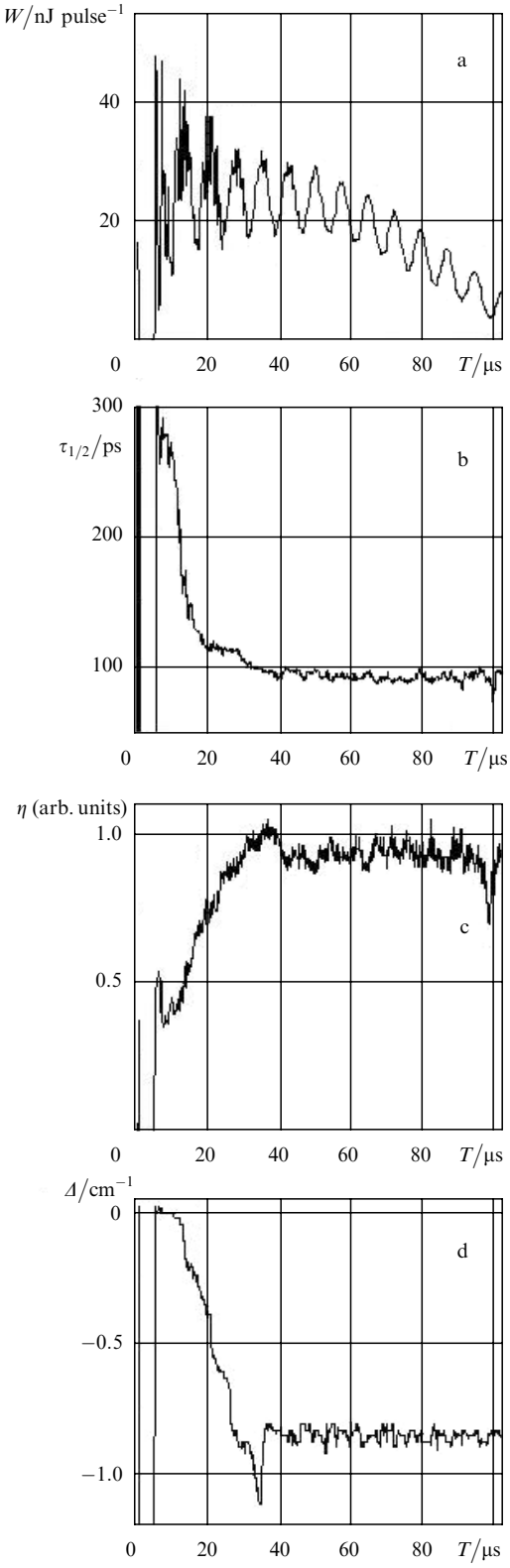

Figure 3. Time dependences of the ultrashort pulse energy (a), the ACF half-width (b), the SHG efficiency (c), and the laser emission spectrum shift (d).

the specification of quite certain distributions of the amplitudes of noise bursts and intervals between them, which contradicts in itself to the concept of a normal noise. However, these results can be explained using papers [11 – 14], where the eigenfunctions – 'supermodes' for the field envelope in the resonator with the external modulation of

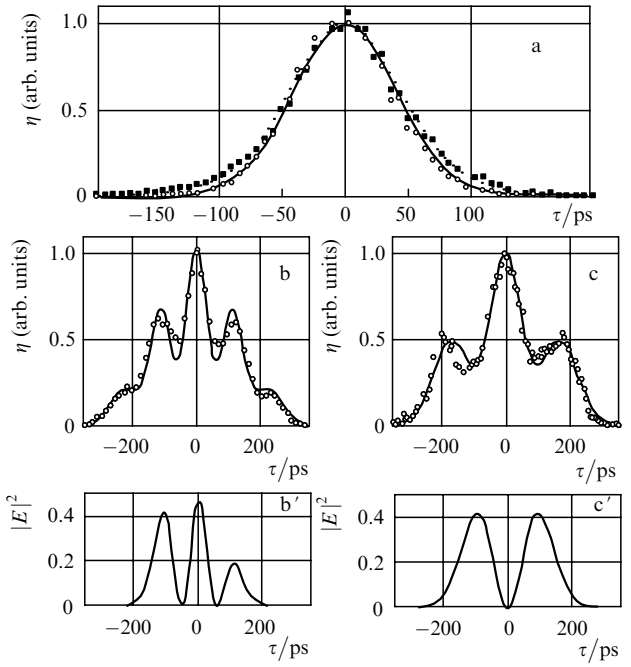

Figure 4. ACF shapes and their approximations by a Gaussian (solid curve) and hyperbolic secant (dashed curve) at $T = 36.5$ (○) and 55 μs (■) (a) and the ACF shapes in the case of excitation of supermodes at $T = 7.2$ μs, $C_0 = 0.22$, $C_1 = 0.22$, $C_2 = -0.95$ (b) and $T = 8$ μs, $C_1 = 1.0$, $C_0 = C_2 = 0$ (c); (b′) and (c′) are the pulse shapes for chosen values of C_k.

losses were obtained in the stationary lasing regime. Supermodes obtained in Refs [11 – 14] by different methods coincide with the eigenfunctions of a harmonic oscillator, in which the time deviation t from the instant of the maximum transmission of a modulator over the modulation period plays the role of a coordinate. The supermodes are described by Hermite polynomials modulated by a Gaussian function

$$A_n(t/\tau_a) = (2^n\sqrt{\pi}n!)^{-1/2} H_n(t/\tau_a) \exp\left[-(t/\tau_a)^2/2\right]. \quad (1)$$

Here, $H_n(x)$ are the nth order Hermite polynomial and $\tau_a = (2g/M\omega_m^2\Omega_g^2)^{1/4}$, where g is the gain for a round trip of a circulating pulse in the resonator, M and ω_m are the modulation degree and frequency, respectively, and Ω_g is the homogeneous width of the gain spectrum.

Note that the formation of pulses corresponding to high-order polynomials was not observed earlier. This can be explained using the results of analysis of the solution stability [14], according to which only the zero-order supermode is stable. If, however, we assume that the high-order supermodes, which decay by the time of the establishment of mode-locking regime, are present in the radiation at the transient stages of the ultrashort pulse formation, then the ACF shape can be quite well described by representing the field in the form of a superposition of Hermitian – Gaussian supermodes

$$E(T,t) = \sum_k C_k(T) A_k(t/\tau_a), \quad (2)$$

where T is the 'slow' time measured in the round-trip transition time in the resonator, and the coefficients $C_k(T)$ satisfy the normalisation condition $\sum_k C_k^2 = 1$.

Examples of the approximation of experimental data taken from the ACF sweeps presented in Fig. 2a are shown in Figs 4b, c, and the pulse shapes used for calculating the ACF are shown in Figs 4b′, c′. In the calculation of the ACF, the parameter τ_a was chosen equal to the FWHM duration of the ultrashort pulse in the stationary regime $\tau_a = \tau_p/[2(\ln 2)^{1/2}]$, i.e., it was not used as a fitting parameter. The coefficients C_k were properly fitted. The development of the algorithm for finding the coefficients would allow a more detailed study of the field evolution, energy exchange between the supermodes, and the decay of high-order supermodes for the entire set of experimental data; however this involves certain difficulties. In addition, eigenfunctions (1) for the field in the resonator are written here for a simplest case, assuming an exact resonance between the modulation and intermode beat frequencies, the coincidence of the lasing frequency with the centre of the homogeneously broadened gain profile, and the absence of gain saturation by an optical pulse after a round trip in the resonator. The consideration of deviations from a simplest approximation leads to the appearance of additional parameters in expression (1) (see, for example, Refs [15, 16]), which further complicates the problem of the regression reconstruction. Although the experimental conditions are beyond the framework of these approximations, the examples considered above confirm quite reliably the involvement of high-order Hermitian – Gaussian supermodes in the formation of ultrashort pulses upon active mode locking.

5. Behaviour of the laser emission spectrum

It was proved or assumed in all the theoretical studies mentioned above that in a laser with active mode locking performed by modulating resonator losses the oscillation occurs at the frequency coincident with the maximum of the gain line of the active medium. However, the behaviour of the laser emission spectrum shown in Figs 2b and 3d cannot be explained by the accepted theory. One can clearly see from these figures that the spectrum gradually shifts to the red, the red shift achieving ~ 0.82 cm^{-1} by the time of the establishment of mode locking. This shift is twice the half-width of the spectral response of the interferometer and is comparable to the linewidth of a Nd : YAG laser.

Note that the frequency calibration was performed by scanning the interferometer between at least two interference maxima, which determined the frequency scale according the known interferometer base equal to 3 ± 0.1 mm. The absolute connection of the frequency axis origin to the centre of the gain band was performed by detecting the integrated emission spectra of the laser. In this case, it was assumed that, in the absence of mode locking, quasi-stationary lasing is observed at the frequency coinciding with the maximum of the gain band.

Figure 5 shows interference patterns obtained for three different regimes: when the mode locker was switched off, when the modulator was switched on at the instant of lasing onset (Figs 2b and 3d), and when the modulator was switched on simultaneously with the flashlamp firing (as in Ref. [8], where no spectral measurements were made). According to the data presented in Figs 2b and 3d, the emission frequency shifts during almost half the lasing time, so that the integrated spectrum in Fig. 5b extends from the

position of free running lasing spectrum (Fig. 5a) to the stationary position of the emission spectrum in the mode locking regime. It follows from Figs 5b and 2b that lasing begins at the maximum of the gain band and then the lasing spectrum shifts to the red and lasing occurs at a shifted frequency. When the modulator is switched on long before the achievement of the lasing threshold, the mode locking regime is established in the process of the below-threshold accumulation of radiation in the resonator, and unshifted fragments of the spectrum are virtually not observed in Fig. 5c. This means that either the spectrum shifts before the achievement of the threshold or it rather rapidly shifts at the leading edge of the envelope of a generated train of ultrashort pulses.

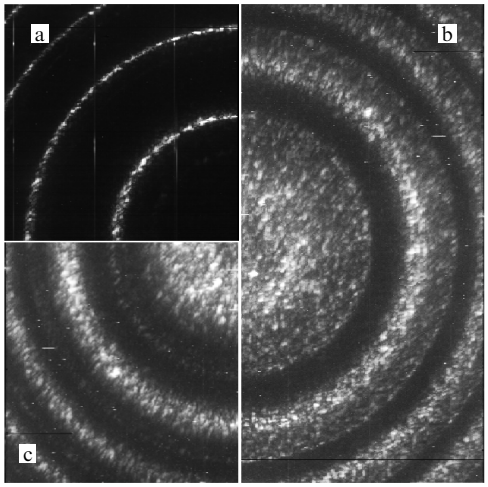

Figure 5. Interference patterns of laser radiation observed when the modulator was switched off (a), when the modulator was switched on after the lasing threshold achievement (b) or simultaneously with the flashlamp firing (c).

Figure 3 shows that there exists a correlation between the rate of the spectral shift of the ultrashort pulse and its energy at the initial stage of lasing. At the maxima of oscillations of the train envelope, the spectral shift rate increases and decreases at the minima. This is probably caused by nonlinear mechanisms of the spectral shift, which produce the rather complicated dynamics of active mode locking. One can see from Fig. 3 that, after several oscillations around the stationary position, the position of the spectrum is finally stabilised despite the remaining oscillations of the lasing envelope. These oscillations of the spectrum upon the transition to the stationary regime are especially distinct in the case of the ultrashort pulse formation before the threshold achievement, when the modulator is switched on simultaneously with the pump pulse (Fig. 6).

It seems that physical mechanisms behind the effects observed can be explained in detail only beyond the scope of approximations used in Refs [1–3, 11–14]. Within the framework of these approximations, the optimal condition upon the modulation of resonator losses is an exact resonance between the modulation and intermode beat frequencies, and upon the phase modulation of radiation in the resonator – the presence of a certain detuning from this resonance [2]. In the latter case, chirped pulses are formed with the spectrum shifted from the gain band

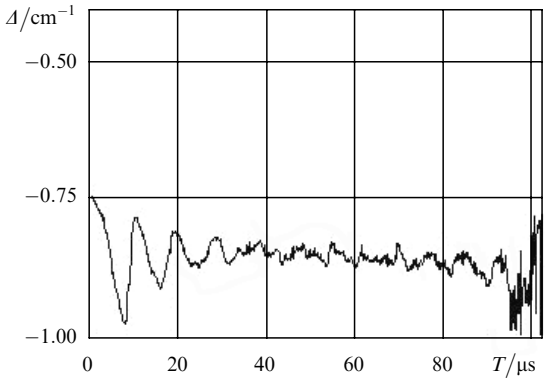

Figure 6. Time dependence of the shift of the emission spectrum upon switching on the modulator simultaneously with the flashlamp firing.

maximum. It was shown in Ref. [15] that in the case of amplitude modulation, the deviation of the modulation frequency from the intermode beat frequency also causes a shift of the ultrashort pulse spectrum. If the gain saturation produced by each individual ultrashort pulse is taken into account, then, as shown in Ref. [16], the effects caused by nonlinearity and group-velocity dispersion come to play, which cause the shift of the optimal modulation frequency with respect to the intermode beat frequency of the resonator. We observed earlier similar effects in the nonstationary regime and simulated them numerically [17, 18]. However, it is hardly possible to explain the results of these spectral measurements using the available papers and a special theoretical treatment is required.

In conclusion of this section, we consider the shape of the spectral response of a scanning interferometer at the beginning of the sweep shown in Fig. 2b. It is well known that the interferometer response for short pulses can be

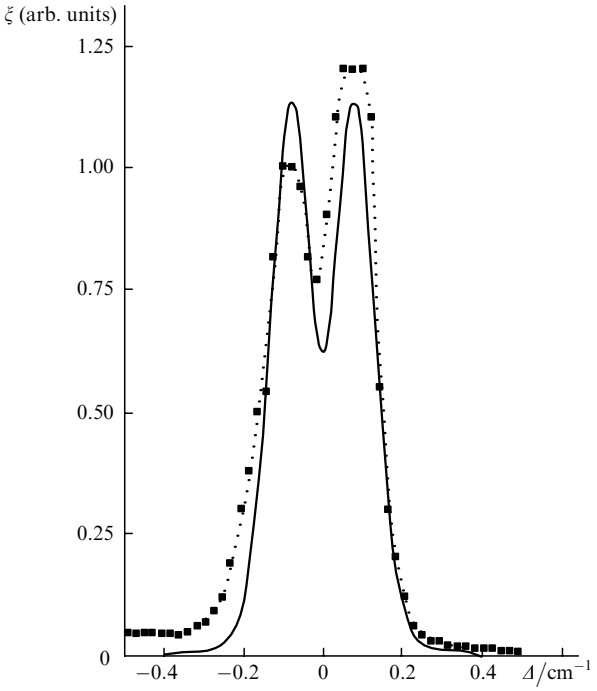

Figure 7. Shape of the interferometer response measured at the beginning of the sweep (■) and its approximation at $C_0 = 0.55$, $C_1 = 0.84$.

directly calculated from the known light-field function [19]. Figure 7 shows the shape of the experimental response observed at the initial stage of mode locking and its approximation with the help of a superposition of the fundamental and first Hermitian–Gaussian supermodes. This approximation well describes the scale and depth of the splitting, which can be interpreted as another evidence of the presence of high-order supermodes in radiation. However, the approximation does not describe the observed asymmetry of the response. Note that similar asymmetric spectral shapes were obtained for the transient regime of active mode locking in numerical calculations within the framework of the spectral-mode representation of the field [20] and taking into account the mismatch between the modulation and intermode beat frequencies [15].

6. Conclusions

The experimental study of the evolution of the ACF and the emission spectrum of a laser with actively modulated resonator losses has shown that mode locking begins with (i) the formation of high-order Hermitian–Gaussian supermodes and is accompanied by the transfer of their energy to the fundamental supermode representing a Gaussian pulse; and (ii) is accompanied by the shift of the laser emission spectrum to the red wing of the gain band.

In addition, in the quasi-stationary regime maintained with the help of a negative feedback, the half-widths of the ACF and spectrum, as well as the position of the spectrum do not change, the regular oscillations of the envelope of the ultrashort pulse train being preserved, i.e., there is no correlation between the ultrashort pulse duration and its energy within the measurement error.

The stationary shape of the ACF, which is close to the shape of a pulse with the envelope described by hyperbolic secant, the shift of the laser emission spectrum with respect to the gain band maximum, and the properties of the transition to the quasi-stationary regime discussed above show that the laser system chooses self-consistently the conditions with dispersion parameters providing such a regime. These facts, showing an important role of dispersion effects, suggest that the observed regime is a quasi-soliton regime, similar to that considered in Refs [21, 22], but it is produced by the internal dispersion and nonlinear properties of the resonator rather than purposely. A weak nonlinearity in this case does not cause the additional shortening of an ultrashort pulse, and a Gaussian supermode and a soliton, which have approximately equal durations, exist by exchanging energy, as in Ref. [21]. However, this assumption should be substantiated in further studies.

References

1. Letokhov V.S. *Zh. Eksp. Teor. Fiz.*, **54**, 1392 (1968).
2. Kuizenga D.J., Siegman A.E. *IEEE J. Quantum Electron.*, **6**, 694 (1970).
3. Kuizenga D.J., Phillion D.W., Lund T., Siegman A.E. *Opt. Commun.*, **9**, 221 (1973).
4. Krivoshchekov G.V., Kulevskii L.A., Nikitin N.G., Semibalamut V.M., Smirnov V.A., Smirnov V.V. *Zh. Eksp. Teor. Fiz.*, **64**, 1997 (1973).
5. Luther-Davies B. *Opt. Commun.*, **57**, 345 (1986).
6. Zaporozhchenko V.A., Kachinskii A.V., Pilipovich I.V., Tylets N.A. *Kvantovaya Elektron.*, **17**, 56 (1990) [*Sov. J. Quantum Electron.*, **20**, 46 (1990)].
7. Zaporozhchenko V.A., Tylets N.A. *Kvantovaya Elektron.*, **23**, 527 (1996) [*Quantum Electron.*, **26**, 512 (1996)].
8. Zaporozhchenko V.A. *Proc. SPIE Int. Soc. Opt. Eng.*, **4353**, 194 (2001).
9. Zaporozhchenko V.A. *Proc. SPIE Int. Soc. Opt. Eng.*, **3682**, 170 (1998).
10. Daussy H., Dumanchin R., de Vitte O. *Appl. Opt.*, **17**, 451 (1978).
11. Haken H., Pauthier M. *IEEE J. Quantum Electron.*, **4**, 454 (1968).
12. Nelson T.J. *IEEE J. Quantum Electron.*, **8**, 29 (1972).
13. Kim D.M., Marathe S., Rabson T.A. *J. Appl. Phys.*, **44**, 1673 (1973).
14. Haus H.A. *IEEE J. Quantum Electron.*, **11**, 323 (1975).
15. Eichler H.J., Koltchanov I.G., Liu B. *Appl. Phys. B*, **61**, 81 (1995).
16. Kalashnikov V.L., Yakovlev V., Apolonski A. *Techn. Digest IQEC 2002* (Moscow: MSU, 2002) p. 447.
17. Zaporozhchenko R.G., Zaporozhchenko V.A., Kondrashov N.G. *Zh. Prikl. Spektrosk.*, **24**, 243 (1976).
18. Apanasevich P.A., Zaporozhchenko R.G., Zaporozhchenko V.A. *Zh. Prikl. Spektrosk.*, **26**, 662 (1977).
19. Babaev V.S., Denchev O., Zhigiliskii A.G., Kuchinskii V.V. *Opt. Spektrosk.*, **54**, 337 (1983).
20. Chong T.W., Lindsay P.A. *Int. J. Electronics*, **45**, 573 (1978).
21. Kartner F.X., Kopf D., Keller U. *J. Opt. Soc. Am. B*, **12**, 486 (1995).
22. Kalashnikov V.L., Kalosha V.P., Poloyko I.G., Mikhailov V.P., Demchuk M.I., Koltchanov I.G., Eichler H.J. *J. Opt. Soc. Am. B*, **12**, 2078 (1995).